

# Lawrence Berkeley National Laboratory

## LBL Publications

### Title

Defining the proteome of human iris, ciliary body, retinal pigment epithelium, and choroid

### Permalink

<https://escholarship.org/uc/item/49h2w0g6>

### Journal

Proteomics, 16(7)

### ISSN

1615-9853

### Authors

Zhang, Pingbo

Kirby, David

Dufresne, Craig

et al.

### Publication Date

2016-04-01

### DOI

10.1002/pmic.201500188

Peer reviewed



# HHS Public Access

Author manuscript

*Proteomics*. Author manuscript; available in PMC 2017 April 01.

Published in final edited form as:

*Proteomics*. 2016 April ; 16(7): 1146–1153. doi:10.1002/pmic.201500188.

## Defining the proteome of human iris, ciliary body, retinal pigment epithelium, and choroid

Pingbo Zhang<sup>1,\*</sup>, David Kirby<sup>1,\*</sup>, Craig Dufresne<sup>2</sup>, Yan Chen<sup>1</sup>, Randi Turner<sup>1</sup>, Sara Ferri<sup>1</sup>, Deepak P. Edward<sup>1,3</sup>, Jennifer E. Van Eyk<sup>4</sup>, and Richard D. Semba<sup>1</sup>

<sup>1</sup>Department of Ophthalmology, Johns Hopkins University School of Medicine, Baltimore, MD

<sup>2</sup>Thermo Fisher Scientific, West Palm Beach, FL

<sup>3</sup>King Khaled Eye Specialist Hospital, Riyadh, Kingdom of Saudi Arabia

<sup>4</sup>Advanced Clinical BioSystems Research Institute, The Heart Institute and Department of Medicine, Cedars-Sinai Medical Center, Los Angeles, CA

### Abstract

The iris is a fine structure that controls the amount of light that enters the eye. The ciliary body controls the shape of the lens and produces aqueous humor. The retinal pigment epithelium and choroid (RPE/choroid) are essential in supporting the retina and absorbing light energy that enters the eye. Proteins were extracted from iris, ciliary body, and RPE/choroid tissues of eyes from five individuals and fractionated using SDS-PAGE. After in-gel digestion, peptides were analyzed using LC-MS/MS on an Orbitrap Elite mass spectrometer. In iris, ciliary body, and RPE/choroid, we identified 2,959, 2,867, and 2,755 non-redundant proteins with peptide and protein false positive rates of <0.1% and <1%, respectively. Forty-three unambiguous protein isoforms were identified in iris, ciliary body, and RPE/choroid. Four “missing proteins” were identified in ciliary body based on 2 proteotypic peptides. The mass spectrometric proteome database of the human iris, ciliary body, and RPE/choroid may serve as a valuable resource for future investigations of the eye in health and disease. The mass spectrometry proteomics data have been deposited to the ProteomeXchange Consortium via the PRIDE partner repository with the dataset identifiers PXD001424 and PXD002194.

### Keywords

Choroid; Ciliary body; Eye; Iris; Retinal Pigment Epithelium

---

The iris controls the amount of light entering the eye by varying pupil size, and also acts as a tissue plane for the anterior chamber. The iris consists of a stroma layer that contains smooth

---

Correspondence: Richard D. Semba, M.D., M.P.H., Wilmer Eye Institute, Smith Building, M015, 400 N. Broadway, Baltimore, MD 21287. Tel. (410) 532-2123, Fax (410) 502-1753, rdsemba@jhmi.edu.

\*These authors contributed equally to the manuscript.

**Abbreviations:** none

The mass spectrometry proteomics data have been deposited to the ProteomeXchange Consortium via the PRIDE partner repository with the dataset identifiers PXD001424 and PXD002194.

Craig Dufresne is an employee of Thermo Fisher Scientific. The remaining authors have declared no conflict of interest.

muscle of the iris sphincter and dilator, extracellular matrix, and blood vessels, and the iris pigmented epithelium. The ciliary body is a ring-shaped tissue that produces aqueous humor and contains the ciliary muscle which controls the shape of the lens. The retinal pigment epithelium (RPE) is a single layer of pigmented cells that provides nourishment for the photoreceptor cells and absorbs light energy that enters the eye [1]. The RPE is involved in phagocytosis of the outer segments of photoreceptors, nutrient transport to and removal of waste products from photoreceptors, and transport and regeneration of retinoids involved in the visual cycle [1]. The RPE also forms the blood/retina barrier. The choroid is a pigmented, thin layer of fenestrated blood vessels that supplies the outer retina. Bruch's membrane separates the RPE from the choroid. The proteome of the human iris, ciliary body, and RPE/choroid require further characterization [2]. The objective of this study was to characterize the proteome of normal human iris, ciliary body, and RPE/choroid complex. These proteomes were grouped together as they comprise the pigmented tissues of the eye.

Five human donor eyes were obtained from the Lions Eye Institute, Tampa, FL. Right eyes were selected from five adults (4 males, 1 female), age 51–76 y, with no history of eye disease or previous eye surgery. The causes of death were myocardial infarction, end-stage renal disease (2), and cancer, not on chemotherapy (2). Time of death to enucleation was 3–7 h for all subjects. Globes were placed in eye bank vials and refrigerated until received at the Wilmer Eye Institute. Time from enucleation to tissue freezing was 24–36 h for all subjects. A corneal surgeon (S.F.) dissected the globes following a standardized protocol for isolation of human eye tissues [3]. Iris was dissected free from ciliary body at its radial edge, taking great care to divide iris and ciliary body. RPE/choroid was dissected free of retina and vitreous. Iris, ciliary body, and RPE/choroid samples were immediately snap frozen and stored at  $-80^{\circ}\text{C}$  until processing. Iris, ciliary body, and RPE/choroid samples were suspended in 1 mL of lysis buffer (10 mM HEPES, 42 mM KCl, 0.1 mM EDTA, 0.1 mM EGTA, 1mM dithiothreitol [DTT],  $1\times$  phosphatase inhibitor [Pierce, PI78420],  $1\times$  protease inhibitor [Sigma, P8340]), and homogenized using a motorized handheld Eppendorf mortar/pestle until tissue was no longer clumped. Samples were then sonicated three times for ten seconds, storing on ice to prevent overheating between sonications. Sodium dodecyl sulfate was added for a final concentration of 2% (w/v). Samples were incubated at room temperature for 10 min to lyse the cells and extract the proteins. The samples were then spun for 45 min,  $14,000\times g$ , at room temperature. Protein concentration of the supernatant was determined using the Pierce microBCA kit.

Proteins were separated using SDS-PAGE 4–12% gradient gels. Double distilled  $\text{H}_2\text{O}$  was added to the samples to achieve 50  $\mu\text{g}$  of protein in 45  $\mu\text{L}$  volume in a low retention Eppendorf tube. Forty-five  $\mu\text{L}$   $4\times$  lithium dodecyl sulfate SE + 100 mM DDT was added to each tube. Tubes were vortexed, spun at 1,000 rpm for 30 sec at room temperature (RT), and placed on a  $106^{\circ}\text{C}$  heat block for 10 min to denature the proteins. Tubes were vortexed and spun twice at 1,000 rpm for 30 second at RT. Fifty  $\mu\text{g}$  of sample was run on each lane of a 1D SDS gel using NuPAGE 4–12% Bis-Tris gel 1.5mm, 200V. Gels were stained with Coomassie blue (250 mL methanol, 50 mL acetic acid, 200 mL  $\text{dH}_2\text{O}$ , 0.5 g Coomassie brilliant blue) at RT for 30 min. Gels were destained (50 mL methanol, 75 mL acetic acid, 875 mL  $\text{dH}_2\text{O}$ ) overnight. Each gel was cut into 12 bands. Gel pieces were placed in separate vials and disrupted with forceps. Gel bands were destained, dehydrated with

acetonitrile, and dried down with an SPD1010 Speedvac concentrator (Thermo Scientific). Samples were reduced with 10 mM DTT for 1 hour at 55°C and alkylated with 55 mM iodoacetamide in 25 mM ammonium bicarbonate for 0.5 hour at RT, washed with ultrapure water, dehydrated with 100% acetonitrile, and dried by Speedvac concentrator. Samples were digested with trypsin/LysC (Promega, V5073 (ratio of protein to enzyme = 50:1) at 37°C overnight with a constant shaking. Supernatant with peptides was collected into a new Eppendorf tube, and the gel slice was incubated with 1% TFA (v/v) in 80% acetonitrile for extracting peptides twice, and then combined all the solution for drying up by Speedvac concentrator. Peptides were resuspended in solvent 0.1% (v/v) formic acid in water (Optima™ LC/MS, Fisher Chemical), desalted by the column (Pierce Spin-Tip), spun, eluted with 0.1% (v/v) formic acid in 80% acetonitrile (Optima™ LC/MS, Fisher Chemical), and then dried by Speedvac concentrator. Samples were resuspended in 0.1% formic acid in water and spiked with 5 fmol/μL calibration peptides (Pierce Peptide Retention Time Calibration Mixture).

Samples were run LC-MS/MS using a one-hour linear gradient B from 2–30% acetonitrile (Fisher Scientific), where buffer A was with 0.1% formic acid and buffer B was 95% acetonitrile and 0.1% formic acid using an EASY-Spray source (Thermo Scientific) coupled with an Orbitrap Elite (Thermo Scientific) mass spectrometer. EASY-Spray source was run at 35°C using a 25 cm x 50 μm integrated spray tip column. Peptides were trapped at 980 bar on a 2 cm x 75 μm trapping column. The trap was a 3 μm particle, and the column was 2 μm Acclaim PepMap C<sub>18</sub>. All individual samples were run with two technical replicates.

MS raw data were batch processed using i3D (Shimadzu and Integrated Analysis), which combines both X!Tandem and OMSSA search engines using the UniProt sequence database (human 2014-12-17.fasta). UniProt database included all human sequences, and parameters allowed for 2 missed tryptic cleavages, a fragment ion mass error of 1 Da, and potential protein modifications for carbamidomethylation, oxidation, phosphorylation, deamidation, and carbamylation. Peptide identifications were accepted if they were established at >90.0% probability by the Peptide Prophet algorithm [4] with Scaffold delta-mass correction. Protein identifications were accepted if they were established at 95.0% probability and contained at least 1 identified proteotypic peptide. Protein Prophet algorithm was used to assign protein probabilities [5] using a false discovery rate (FDR) of <0.1% for peptides and <1.0% for proteins. Proteins that contained the same peptides but could not be differentiated based on MS/MS analysis alone were grouped to satisfy the principles of parsimony. Proteins sharing significant peptide evidence were grouped into clusters.

In iris, a total of 19,988 peptides were identified, resulting in 2,959 non-redundant proteins identified (Supporting Tables 1 and 2). The percentage of all the 2,959 proteins that were identified on the basis of a match of 5, 4, 3, 2, peptides and 1 peptide was 43.5%, 9.2%, 12.0%, 16.1%, and 19.2%, respectively. In ciliary body, a total of 18,684 peptides were identified, resulting in 2,867 non-redundant proteins identified (Supporting Tables 3 and 4). The percentage of 2,867 proteins that were identified on the basis of a match of 5, 4, 3, 2, peptides and 1 peptide was 43.9%, 9.3%, 12.1%, 17.3%, and 17.4%, respectively. In RPE/choroid, a total of 17,865 peptides were identified, resulting in 2,755 non-redundant proteins identified in the normal human RPE/choroid (Supporting Tables 5 and 6). The percentage of

2,755 proteins that were identified on the basis of a match of 5, 4, 3, 2, peptides and 1 peptide was 43.8%, 8.7%, 11.6%, 16.6%, and 19.3%, respectively

For peptides used to identify proteins on the basis of a single peptide, MS/MS spectra were manually validated and submitted to ProteomeXchange via PRIDE with the identifiers PXD001424 and PXD002194. A scatterplot of spectral count/molecular weight for each protein versus number of distinct peptides is shown separately for iris, ciliary body, and RPE/choroid (Supporting Figure 1). Protein isoforms were further confirmed following observation of the putative isoforms from the i3D data search and processing. Peptide amino acid sequences compared with sequence alignment of the different isoforms in order to confirm unambiguous identification of a peptide to a sequence unique to an isoform and the quality of the spectra manually verified. There were 43 unambiguous protein isoforms identified in human iris, ciliary body, and RPE/choroid (Table 1). Seven protein isoforms were annotated on UniProt as previously lacking confirmation of existence at the protein level. PANTHER analysis was used to classify protein function [6] in iris, ciliary body, and RPE/choroid, respectively (Figures 1a–c).

The overlap between the 2,959 iris proteins with 465 previously published proteins identified in the aqueous humor using proteomic and mass spectrometry approaches [2], and 3,677 plasma proteins in the Plasma Peptide Atlas [7], and 465 previously published aqueous humor proteins are shown in Supporting Figure 2a. The overlap between the 2,867 ciliary body proteins described in the present study, 3,677 plasma proteins, and 2,782 previously published ciliary body proteins [8] is shown in Figure 2b. The overlap between 2,755 RPE/choroid proteins in the present study, 3,677 plasma proteins, and 897 previously published RPE/choroid proteins [2] is shown in Figure 2c.

Four examples of MS/MS spectra of peptides used for identification of proteins in the human iris are shown in Supporting Figure 3a. There were four “missing proteins” [9] found in ciliary body: (1) putative coiled-coil-helix-coiled-coil-helix domain-containing protein CHCHD2P9, mitochondrial, (2) microtubule-associated proteins 1A/1B light chain 3 beta 2, (3) putative small nuclear ribonucleoprotein G-like protein 15, and (4) putative keratin-87 protein. The “missing proteins” are those in neXtProt annotated for documented existence as “uncertain” or “transcript level evidence”. All MS/MS spectra for peptides used to identify the “missing proteins” are shown in Supporting Figure 3b. Four examples of MS/MS spectra of peptides used for identification of CD antigens and other proteins in RPE/choroid are shown in Figure 3c.

Separate heat maps of the total unique peptides in human iris, ciliary body, and RPE/choroid are presented in Supporting Figure 4. The proteins found in iris, ciliary body, and RPE/choroid, respectively, were compared with the Human Peptide Atlas in Supporting Figure 5. The proteins found in iris, ciliary body, and RPE/choroid, respectively are compared with kidney and urine proteomes [10] in Supporting Figure 6. We compared the proteins identified in the RPE/choroid with a recent curated list of genes associated with age-related macular degeneration (AMD) [10]. There were 189 proteins in the RPE/choroid that have been associated with AMD (Supporting Table 7). A semi-quantitative comparison of proteins across iris, ciliary body, and RPE/choroid is provided in Supporting Table 8.

The iris contained many myosins and tropomyosins related to motor function, proteins related to melanin pigmentation, many collagens and matrix proteins, and numerous selenoproteins. The ciliary body also contained many myosins, unconventional myosins, and tropomyosins, which are related to the ciliary muscle that controls the shape of the lens during accommodation. The RPE/choroid contained many enzymes involved in the visual cycle and retinoid metabolism, growth factors, proteins in the complement pathway, and several apolipoproteins.

## Supplementary Material

Refer to Web version on PubMed Central for supplementary material.

## Acknowledgments

This work was supported by the National Institutes of Health grants R01 EY024596, R01 AG027012, NHLBI proteomics contract NHLBI-HV-10-05 (2) (JVE), the Joint King Khaled Eye Specialist Hospital and Wilmer Eye Institute Research Grant Program, the Edward N. & Della L. Thome Memorial Foundation, and Research to Prevent Blindness.

## References

1. Strauss O. The retinal pigment epithelium in visual function. *Physiol Rev.* 2005; 85:845–881. [PubMed: 15987797]
2. Semba RD, Enghild JJ, Venkatraman V, Dyrland TF, Van Eyk JE. The Human Eye Proteome Project: perspectives on an emerging proteome. *Proteomics.* 2013; 13:2500–2511. [PubMed: 23749747]
3. Skeie JM, Mahajan VB. Dissection of human vitreous body elements for proteomic analysis. *J Vis Exp.* 2011; 47:e2455.
4. Keller A, Nesvizhskii AI, Kolker E, Aebersold R. Empirical statistical model to estimate the accuracy of peptide identifications made by MS/MS and database search. *Anal Chem.* 2002; 74:5383–5392. [PubMed: 12403597]
5. Nesvizhskii AI, Keller A, Kolker E, Aebersold R. A statistical model for identifying proteins by tandem mass spectrometry. *Anal Chem.* 2003; 75:4646–4658. [PubMed: 14632076]
6. Mi H, Muruganujan A, Casagrande JT, Thomas PD. Large-scale gene function analysis with the PANTHER classification system. *Nat Protoc.* 2013; 8:1551–1566. [PubMed: 23868073]
7. Farrah T, Deutsch EW, Omenn GS, Sun Z, Watts JD, Yamamoto T, Shteynberg D, Harris MM, Moritz RL. State of the human proteome in 2013 as viewed through PeptideAtlas: comparing the kidney, urine, and plasma proteomes for the biology- and disease-driven Human Proteome Project. *J Proteome Res.* 2014; 13:60–75. [PubMed: 24261998]
8. Goel R, Murthy KR, Srikanth SM, Pinto SM, Bhattacharjee M, Kelkar DS, Madugundu AK, Dey G, Mohan SS, Krishna V, Prasad TSK, Chakravarti S, Harsha HC, Pandey A. Characterizing the normal proteome of human ciliary body. *Clin Proteomics.* 2013; 10:9. [PubMed: 23914977]
9. Lane L, Bairoch A, Beavis RC, Deutsch EW, Gaudet P, Lundberg E, Omenn GS. Metrics for the Human Proteome Project 2013–2014 and strategies for finding missing proteins. *J Proteome Res.* 2014; 13:15–20. [PubMed: 24364385]
10. Newman AM, Gallo NB, Hancox LS, Miller NJ, Radeke CM, Maloney MA, Cooper JB, Hageman GS, Anderson DH, Johnson LV, Radeke MJ. Systems-level analysis of age-related macular degeneration reveals global biomarkers and phenotype-specific functional networks. *Genome Med.* 2012; 4:16. [PubMed: 22364233]

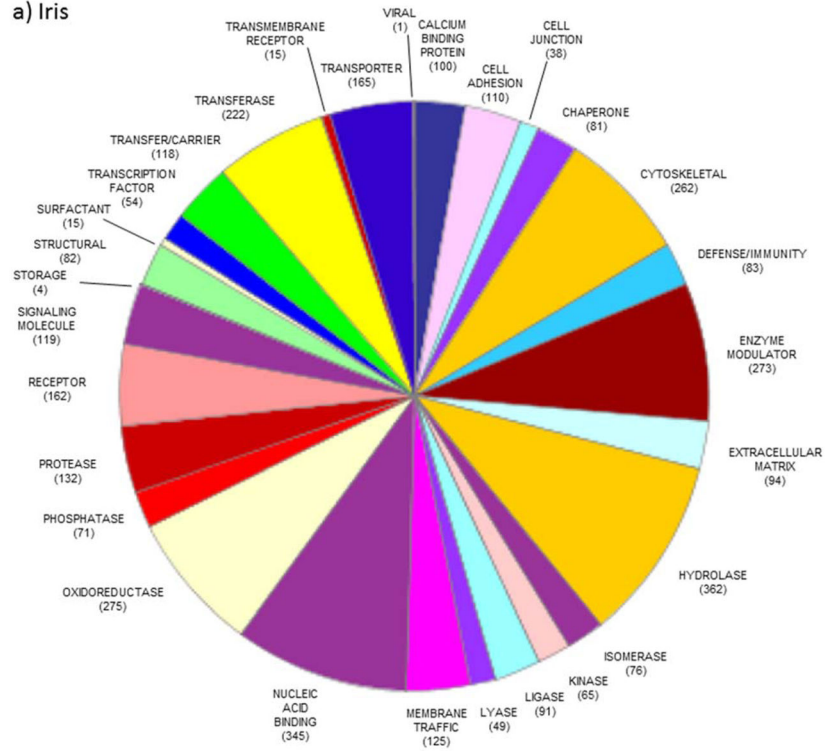
Author Manuscript

Author Manuscript

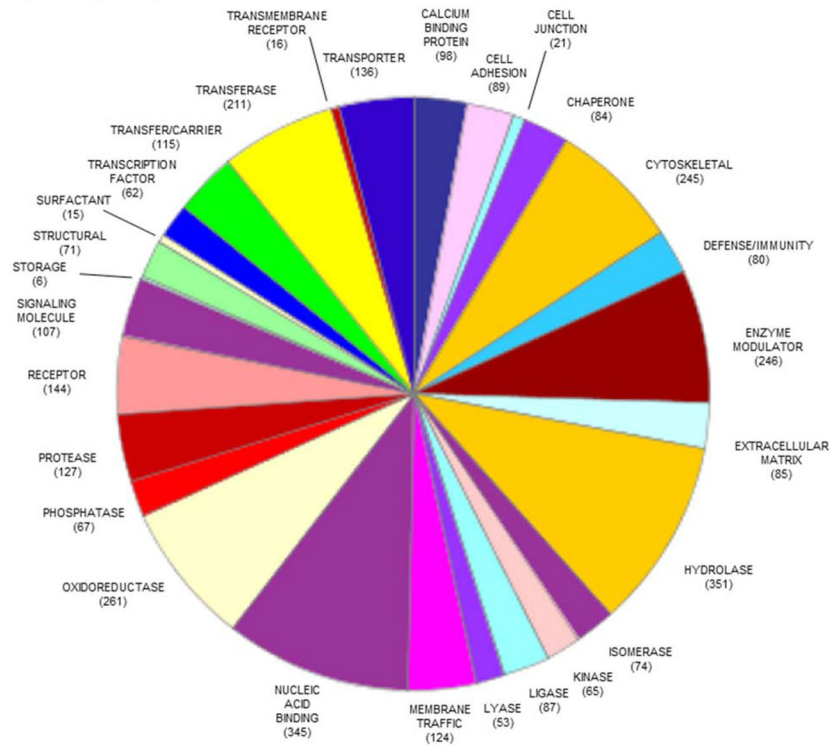
Author Manuscript

Author Manuscript

a) Iris



b) Ciliary body



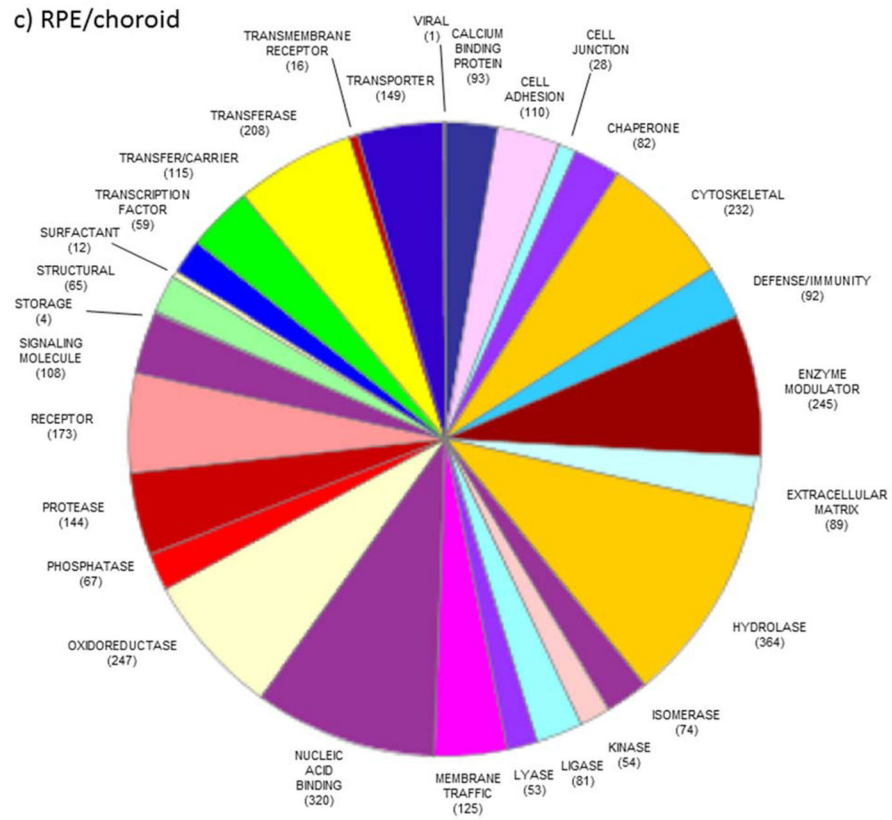


**Figure 1.** Pie diagram of the distribution of protein functions in the iris (a), ciliary body (b), and RPE/choroid (c) according to their molecular functions as determined using PANTHER.



Table 1

Forty-three unambiguous protein isoforms identified in human iris, ciliary body, and RPE/choroid. All isoforms are products of alternative splicing.

UniProt ID	Protein Name	Distinguishing Peptide(s)	Protein Function/	Tissue <sup>2</sup>		
				Iris	Ciliary body	RPE/choroid
Q15147-4*	1-phosphatidylinositol 4,5-bisphosphate phosphodiesterase beta-4, isoform 3	SCHAVSQTQEGGDAADGEIGSR	role in signal transduction		x	
P51178-2*	1-phosphatidylinositol 4,5-bisphosphate phosphodiesterase delta-1, isoform 2	LGLQDDEDLQALLK	mediates production of diacylglycerol and inositol 1,4,5-triphosphate	x		
O00468-6	Agtrin, isoform 6	TFVEYLNVAVTESEK	isoform 6 may be involved in endothelial cell differentiation	x		
Q9NV17-2	ATPase family AAA domain-containing protein 3A, isoform 2	LKEYEAAVEQLK	essential for mitochondrial network organization, mitochondrial metabolism and cell growth at organism and cellular level		x	
Q96LW7-2	Bcl10-interacting CARD protein, isoform 2	VLGFSVPVHDR	inhibits effects of BCL10-induced activation of NF-kappaB	x	x	x
Q92843-2*	Bcl-2-like protein 2, isoform 3	TSLALDESLFR	promotes cell survival		x	
P60953-1	Cell division control protein 42 homolog, isoform 1	YVECSALTQR	plasma membrane-associated small GTPase		x	x
P09496-2	Clathrin light chain A, isoform Non-brain	AAEAFVNDIDESSPGTEWER	major protein of the polyhedral coat of coated pits and vesicles	x		
O75367-2	Core histone macro-H2A.1, isoform 1	LQVVQADIASIDSDAVVHPTNTDFYIGGEGVNTLEK	variant histone H2A that replaces conventional H2A in a subset of nucleosomes where it represses transcription		x	
Q14195-2	Dihydropyrimidinase-related protein 3, isoform LCRMP-4	EVLQNLGPK EPAPASPAPAGVEIR TLDFDALSVQR EESREPAPASPAPAGVEIR	necessary for signaling by class 3 semaphorins and subsequent remodeling of cytoskeleton	x	x	x
Q9NRG7-2	Epimerase family protein SDR39U1, isoform 2	GHEVTLVSR	putative NADP-dependent oxidoreductase.		x	
Q9BSJ8-2*	Extended synaptotagmin-1, isoform 2	AQDLPMVTSELYPPQLK	binds glycerophospholipids in a barrel-like domain	x		
P47756-2	F-actin-capping protein subunit beta, isoform 2	NDLVEALK NDLVEALKR SVQTFADK	binds in a Ca <sup>2+</sup> independent manner to fast growing ends of actin filaments	x	x	x
P23142-4	Fibulin-1, isoform C	HGTVSSFVAK	incorporated into fibronectin-containing matrix fibers	x		

UniProt ID	Protein Name	Distinguishing Peptide(s)	Protein Function <sup>1</sup>	Tissue <sup>2</sup>		
				Iris	Ciliary body	RPE/choroid
Q96BI3-3	Gamma-secretase subunit APH-1A, isoform 3	VIIIVAGR	essential subunit of the gamma-secretase complex	x		
O94925-3	Glutaminase kidney, isoform, isoform 3, mitochondrial	HSFGPLDYESLQQELALK VSPESNEDISTTVVYR	maintains acid-base homeostasis; isoform 3 activated by phosphate	x	x	
P01116-2	GTPase Kras, isoform 2B	QGVDDAFYTLVR	binds GDP/GTP and possesses intrinsic GTPase activity	x	x	x
P09471-2	Guanine nucleotide-binding protein G(o) subunit alpha, isoform Alpha-2	LFDSICNKK	involved as modulator or transducer in various transmembrane signaling systems	x		
Q70UQ0-4	Inhibitor of nuclear factor kappa-B kinase-interacting protein, isoform 4	TLEGIQYDNSILK	target of p53/TP53 with pro-apoptotic function			x
P31994-2	Low affinity immunoglobulin gamma Fc region receptor II-b, isoform IIB2	ISANPTNPDEADK	involved in a variety of effector and regulatory functions such as phagocytosis of immune complexes and modulation of antibody production by B-cells		x	
P51608-2	Methyl-CpG-binding protein 2, isoform B	AAAAAAAAPSGGGGGEEERLEEK	chromosomal protein that binds to methylated DNA	x		
Q16891-2	Mitochondrial inner membrane protein, isoform 2	GDPASATAGDTLSPAPAVQPEESLK	mitochondrial calcium ion homeostasis	x	x	
Q9NYL2-2	Mitogen-activated protein kinase kinase kinase MLL1, isoform 2	LTEQSNTPLLPLAAR	stress-activated component of a protein kinase signal transduction cascade		x	
P25189-2	Myelin protein P0, isoform L-MPZ	VMVIEIELR	creation of an extracellular matrix face			x
P35749-2	Myosin-11, isoform 2	GNETSFVPSR KDTSIITQGPSFAYGELEK DTSITQGPSFAYGELEK	muscle contraction		x	
P56181-2	NADH dehydrogenase [ubiquinone] flavoprotein 3, isoform 2, mitochondrial	LLATQTAAELSK VASPSPSGSVLFTDEGVPK	accessory subunit of the mitochondrial membrane respiratory chain NADH dehydrogenase (Complex I)	x		
Q14697-2	Neutral alpha-glucosidase AB, isoform 2	VNLTLSGIWDK	cleaves sequentially the 2 innermost alpha-1,3-linked glucose residues from the Glc(2)Man(9)GlcNAc(2) oligosaccharide precursor of immature glycoproteins	x	x	
Q8N490-2	Probable hydrolase PNKD, isoform 2	LSNTGYESQR ASSQSAPSPDVGSGVQT	plays a role in the development of cardiac hypertrophy via activation of the NF-kappa-B signaling pathway	x	x	

UniProt ID	Protein Name	Distinguishing Peptide(s)	Protein Function <sup>1</sup>	Tissue <sup>2</sup>		
				Iris	Ciliary body	RPE/choroid
P14618-2	Pyruvate kinase isozymes M1/M2, isoform M1	CLAAALIVLTESGR KLFEEELVLR LFEELVLR EAEAAMFHR	catalyzes the transfer of a phosphoryl group from phosphoenolpyruvate (PEP) to ADP, generating ATP; M1 is the main form in muscle, heart and brain	x	x	x
Q16799-3	Reticulon-1, isoform RTN1-C	SQAIDLLYWR MDCVVWSNWK	may be involved in neuroendocrine secretion or in membrane trafficking in neuroendocrine cells	x	x	x
Q9NQC3-3	Reticulon-4, isoform 3	DKVVLDLYWR VVLDLYWR	developmental neurite growth regulatory factor; isoform 3 inhibits BACE1 activity and amyloid precursor protein processing	x		x
Q9NQC3-5	Reticulon-4, isoform 5	GSSGSVVVDLLYWR SSAVVDLLYWR	developmental neurite growth regulatory factor	x	x	
O94875-2	Sorbin and SH3 domain-containing protein 2, isoform 2	INPDDIDLENEPWPYK	adapter protein that plays a role in the assembling of signaling complexes, being a link between ABL kinases and actin cytoskeleton.		x	
P16615-2	Sarcoplasmic/endoplasmic reticulum calcium ATPase 2, isoform 2	NYLEPAILE	catalyzes the hydrolysis of ATP coupled with the translocation of calcium from the cytosol to the sarcoplasmic reticulum lumen; isoform 2 is involved in the regulation of the contraction/relaxation cycle	x	x	
P16615-3	Sarcoplasmic/endoplasmic reticulum calcium ATPase 2, isoform 3	NYLEPVLSEL	catalyzes the hydrolysis of ATP coupled with the translocation of calcium from the cytosol to the sarcoplasmic reticulum lumen	x		
Q13813-2	Spectrin alpha chain, non-erythrocytic 1, isoform 2	LQTASDES YKDPNTNQLSK	interacts with calmodulin in a calcium-dependent manner	x		
Q13813-3	Spectrin alpha chain, non-erythrocytic 1, isoform 3	QEIQDNQYHSLLELGEK	interacts with calmodulin in a calcium-dependent manner	x	x	
Q8TBG9-2*	Synaptotagmin, isoform 2	MDPVSQLASACTFR	intrinsic membrane protein of small synaptic vesicles			x
Q5ITV8-3*	Torsin-1A-interacting protein 1, isoform 3	SIQEAPAVSEDLVIR	plasma membrane-associated small GTPase which cycles between an active GTP-bound and an inactive GDP-bound state		x	
O14787-2*	Transportin-2, isoform 2	TLLNTAITIGR	probably functions in nuclear protein import as a nuclear transport receptor			x
P67936-2	Tropomyosin alpha-4 chain, isoform 2	ASDAEGDVAALNR	plays a central role, in association with the troponin complex, in the calcium dependent regulation of vertebrate striated muscle contraction		x	
P07951-2	Tropomyosin beta chain, isoform 2	SLMASEEYSTK TIDDLLEETLASAK	binds to actin filaments in muscle and non-muscle cells			x

UniProt ID	Protein Name	Distinguishing Peptide(s)	Protein Function <sup>1</sup>	Tissue <sup>2</sup>		
				Iris	Ciliary body	RPE/choroid
Q9Y277-2	Voltage-dependent anion-selective channel protein 3, isoform 2	SCSGVMEFSTSGHAYTDIGK	forms a channel through the mitochondrial outer membrane that allows diffusion of small hydrophilic molecules		x	

\*UniProt website (<https://www.uniprot.com>) noted for the specific isoform that "No experimental confirmation available" (01/15/15)

<sup>1</sup>Protein function based upon neXtProt. If information available on function for specific isoform, this is also specified.

<sup>2</sup>CB = ciliary body; R/C = RPE/choroid